Mater. Res. Soc. Symp. Proc. Vol. 1463 © 2012 Materials Research Society
DOI: 10.1557/opl.2012.1073

Improved Temperature Stability of Atomic Layer Deposition Coated Cellulose Nanocrystal Aerogels

Sean W. Smith,[1] Han Chan,[2] Christian Buesch,[3] John Simonsen,[2] and John F. Conley Jr.[1]

[1]School of Electrical Engineering and Computer Science, Oregon State University, 1148 Kelley Engineering Center, Corvallis, OR 97331, U.S.A.

[2]Wood Science and Engineering, Oregon State University, 119 Richardson Hall, Corvallis, OR 97331, U.S.A.

[3]School of Mechanical, Industrial, and Manufacturing Engineering, Oregon State University, 204 Rogers Hall, Corvallis, OR 97331, U.S.A.

ABSTRACT

Atomic layer deposition (ALD) was used to coat cellulose nanocrystal (CNC) aerogel scaffolds with a thin conformal layer of Al_2O_3. Electron probe microanalysis indicates that the penetration of Al_2O_3 into the aerogel was greater than 50 μm. Thermogravimetric analysis (TGA) shows that Al_2O_3 coated CNC aerogel composites have improved temperature and oxidation resistance.

INTRODUCTION

An aerogel is a sol gel in which the liquid solvent has been replaced by air without collapsing the suspension, creating a unique microstructure of loosely spaced fibres with very high porosity, low density, and high surface area [1]. CNCs are a renewable material with mechanical properties comparable with carbon fiber, making CNC aerogels attractive as a low cost renewable alternative for fiber reinforced polymers with potential applications such as plastic casings for cell phones and laptops [1]. However, the sensitivity of CNC aerogels to oxidation limits their ability to be incorporated into polymers which require high temperature processing (>200 °C) in oxygen containing environments [1].

ALD allows surface limited deposition of highly uniform and conformal thin films of inorganic oxides over high aspect ratio porous and large surface area structures. ALD Al_2O_3 layers as thin as 25 nm make excellent moisture permeation barriers [2]. ALD is a chemical vapor deposition like method in which the reactants are alternately dosed to the substrate, limiting the reaction to a chemisorbed surface layer. An ALD cycle consists of 4 basic steps: (1) A pulse of the first reactant is introduced; (2) Reaction products and excess reactants are purged away with an inert gas (N_2); (3) A pulse of the second reactant is introduced which reacts with the chemisorbed layer of the first reactant; (4) Excess reactant and reaction products are purged away with inert gas (N_2). These 4 steps are repeated to deposit a film of desired thickness.

In this work, ALD is used to deposit conformal Al_2O_3 coatings on CNC aerogels. In order to coat a high aspect ratio structure such as an aerogel, the four steps described above are modified. After steps (1) and (3), additional exposure steps are added during which the substrate is allowed to soak in the reactant gasses to allow the reactants time to diffuse into the porous substrate. Similarly the purge step is extended to give the excess reactants and reaction products time to diffuse out again. Finally, a larger dose of reactant must often be used (by increasing the

pulse time) to account for the high surface area of the aerogel and provide a larger driving force for diffusion into the aerogel [4-9].

The preliminary work described here is directed towards investigating the feasibility of protecting CNC aerogels from oxidation by coating with a conformal Al_2O_3 diffusion barrier. The effect of ALD pulse time and exposure / purge time was investigated. Electron probe microanalysis (EPMA) was used to measure Al penetration into the aerogel. SEM was used to monitor coating conformality and coated aerogel microstructure. TGA was used to assess the effectiveness of the coatings in protecting the aerogels and preventing oxidation related weight loss.

EXPERIMENTAL DETAILS

CNCs were prepared from pure cotton cellulose by sulfuric acid hydrolysis using a previously described method [10]. The resulting aqueous CNC dispersion was then subjected to oxidation, converting the surface C6 primary hydroxyls to carboxylic acids via (2,2,6,6-tetramethylpiperidin-1-yl)oxyl (TEMPO) mediated carboxylation [11-14]. Briefly, 200 mL of 1% CNC suspension was slowly stirred with 140 mg of TEMPO (70 mg/g CNC) and 360 mg of NaBr (180 mg/g CNC). The reaction was initiated by adding an initial 10 mL of 11% hypochlorite (NaClO) to the reaction mixture. A pH of 10.2 to 10.5 was maintained by adding dilute NaOH via a pH controller for 48 hrs. The reaction was quenched with 30 to 40 mL of ethanol and then purified by dialysis. Carboxylate content on the CNC surface was determined via potentiometric titration against 0.05 N NaOH.

Al_2O_3 was deposited on approximately 10 mm x 5 mm x 5 mm aerogel pieces via ALD using trimethylaluminium (TMA, $Al(CH_3)_3$) and water as reactants. Films were deposited in a Gemstar Arradiance flow-through hot wall reactor at 150°C. To reduce absorbed water, aerogels were baked out in the deposition chamber at 150°C and ~ 1 Torr N_2 for 30 min. prior to deposition. In order to allow additional time for reactants to diffuse in and out of this 3D high surface area substrate, reactant exposure steps were added to the typical ALD cycle. An ALD cycle in this work thus consists of a TMA pulse / exposure / N_2 purge / H_2O pulse / exposure / N_2 purge. Prior to the pulse, the pump line is closed. The reactants are pulsed into the closed chamber and during the exposure step the sample is allowed to soak in the reactant gasses. Depositions of 50 ALD cycles and 272 ALD cycles were used with a range of precursor pulse times (20, 60, 180 ms) and exposure / purge times (30, 120, 600 s). Note that the exposure and purge times are set equal.

Al_2O_3 film thickness was measured via ellipsometry. Control samples deposited on planar silicon substrates showed the 50 cycle films to be about 8 nm thick and the 272 cycle films about 40 nm thick. To investigate Al_2O_3 penetration, EPMA using a Cameca SX-100 Electron Microprobe was performed on Al_2O_3 coated aerogel samples that were first embedded in polymer, cross sectioned, and then polished. To examine the microstructure as well as Al_2O_3 penetration, other coated aerogels were cracked in half and the fracture surface examined using either an FEI QUANTA 3D dual beam SEM/FIB or an FEI NOVA NanoSEM 230 high resolution SEM. Weight loss curves of coated and uncoated aerogels were collected in a TA Instruments TGA Q500 thermogravimetric analyzer.

RESULTS AND DISCUSSION

Electron Microprobe Analysis

Shown in Figure 1 is an EPMA image of an aerogel coated with 50 cycles of Al_2O_3 using 20 ms pulses with 120 s exposures and purges. The image shows about 60 µm of Al_2O_3 penetration into the interior of the aerogel. There appear to be two distinct regions, an outer layer with high Al_2O_3 counts and an inner layer with less Al_2O_3.

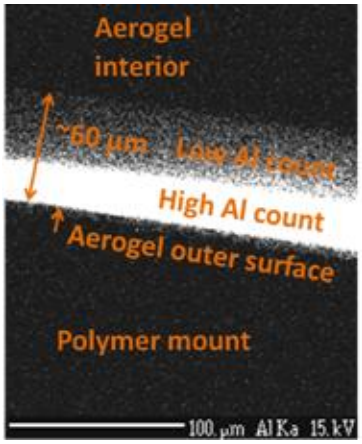

Figure 1: EPMA image of an aerogel coated with 50 ALD cycles consisting of 20 ms pulses with 120 s exposures and purges.

Shown in Figure 2 (a) and (b) are EPMA images of two different regions of an aerogel coated with 50 cycles of Al_2O_3 using 20 ms pulses with exposures and purges *increased* to 600 s. In Figure 2(a), the coating penetrates about 75 µm into the aerogel while in Figure 2(b) it penetrates only about 40 µm. Figure 2(c) is a back scatter electron image showing the regions where scans in Figure 2(a) and 2(b) were taken. One explanation for the observed variation in penetration depth is variation in the microstructure of the sample along the surface – if some regions are more open they may be more easily penetrated. Another explanation could be that the angle of the cleaved face with respect to the surface is not the same for all regions of the surface. Future work will focus on determining Al_2O_3 penetration as a function of aerogel porosity.

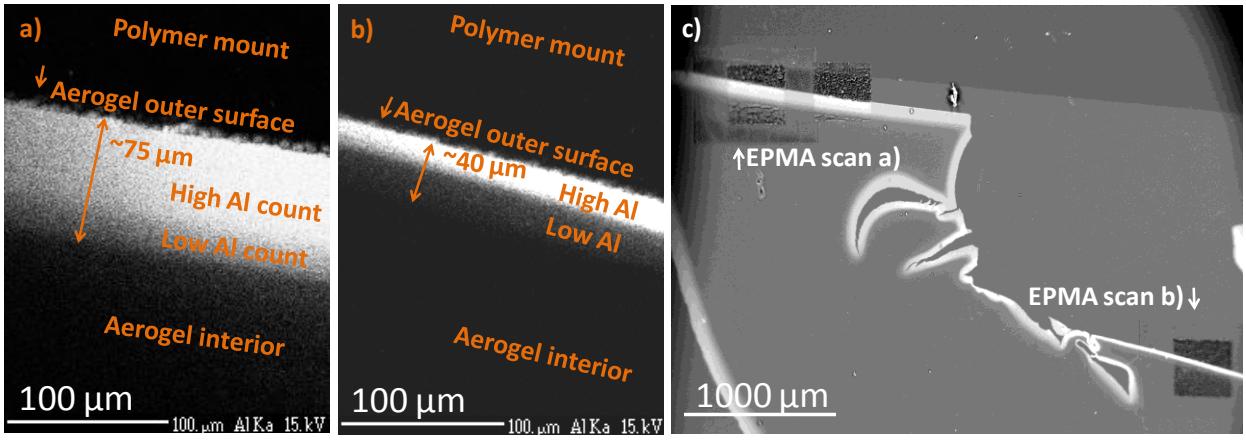

Figure 2: (a,b) EPMA images and (c) a back scatter electron image, for an aerogel sample coated with 50 ALD cycles consisting of 20 ms pulses with 600 s exposures and N_2 purges.

In both Figures 1 and 2, two regions of Al intensity are visible, a region of high Al intensity near the surface and a region of low Al intensity towards the interior. Comparing Figure 2(a) with Figure 1, it appears that these depositions are reactant limited since the added 480 s of exposure and purge time did little to improve the penetration depth. TGA data presented below help to provide further clarification.

Scanning Electron Microscope

Shown in Figure 3 are SEM images of the outer Al_2O_3 rich region of the cross section of an aerogel coated with 272 ALD cycles with 60 ms pulses and 120 s exposure and purges. The cross section was formed by snapping the coated aerogel into two pieces. As shown in the lower resolution image, Figure 3(a), coated aerogel samples typically fracture along a surface that coincides with the transition between high and low Al intensity. The fracture surface appears to be created due to the preferential propagation of the fracture along the boundary between the stiffer Al_2O_3 rich surface region and the more ductile Al_2O_3 free center of the aerogel. As shown in Figure 3(b), there does not appear to be any sharp change in the microstructure that would abruptly limit ALD reactant penetration.

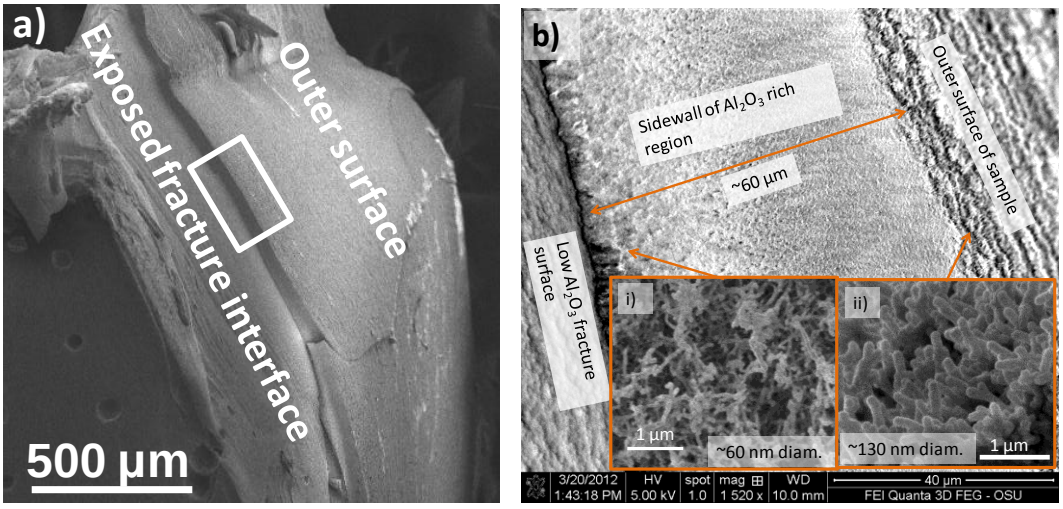

Figure 3: (a) low and (b) high resolution SEM images of Al_2O_3 rich outer surface of a fractured Al_2O_3 coated aerogel with 272 cycles of 60 ms pulses and 120 s exposures and purges. Image (b) corresponds to region in white box shown in (a). Insets show higher magnification SEM images of fibers (i) near the bottom and (ii) at the surface of the Al_2O_3 rich region.

Higher magnification images in the insets indicate that (i) the coated fibers near the fracture are approximately 60 nm in diameter and (ii) the coated fibers near the surface are approximately 130 nm in diameter. A planar silicon control included in the same run had an Al_2O_3 thickness of 45 nm. Uncoated CNCs have diameters around 10 nm. Thus, the fibers near the fracture are coated with approximately 25 nm of Al_2O_3, about 20 nm less than the planar control. On the other hand, the fibers near the outer surface have approximately 60 nm of Al_2O_3 coating, about 15 nm excess over the planar control. Other groups coating similarly formed CNC aerogels have reported an excess coating thickness over the planar control, but typically of only 2

to 7 nm [4-9]. This suggests that the 30 min, 150 °C bake used in this study prior to ALD deposition was not sufficient to completely remove all H_2O.

Thermogravimetric Analysis

TGA weight loss measurements conducted in air at a ramp rate of 10°C/min were used to evaluate the effectiveness of Al_2O_3 coatings in preventing weight loss. In Figure 4(a) is a plot of the weight % vs. temperature for a number of different Al_2O_3 deposition conditions. In general, it is seen that weight loss is reduced as the pulse time (dose) and exposure/purge times (diffusion time) are increased. Part of the reason for this is that as the aerogels become more fully coated with Al_2O_3, a larger fraction of their total mass is composed of noncombustible Al_2O_3. To determine whether the Al_2O_3 coating is actually protecting the aerogel from oxidation, a plot of the differential weight % vs. temperature for the same data is shown in Figure 4(b). The peaks on each differential curve indicate the temperature at which weight loss occurs most rapidly. For all coated aerogels, the weight loss peak occurs at a higher temperature than in the uncoated aerogel, indicating that the Al_2O_3 coating does indeed protect the aerogel against oxidation. As pulse and exposure/purge times are increased, the weight loss peak moves to higher temperatures indicating that as more of the aerogel is coated, the CNC weight loss is delayed to higher temperatures.

Note that depending on the pulse/exposure/purge time combination, ALD may be either dose or diffusion time limited. For example, for fixed 120 s exposure and purge times, the 180 ms pulse shows no improvement over the 60 ms pulse, suggesting that diffusion time is limiting the deposition. However, increasing the exposure/purge times to 600 s for the same 180 ms pulse results in a large increase in the peak weight loss temperature.

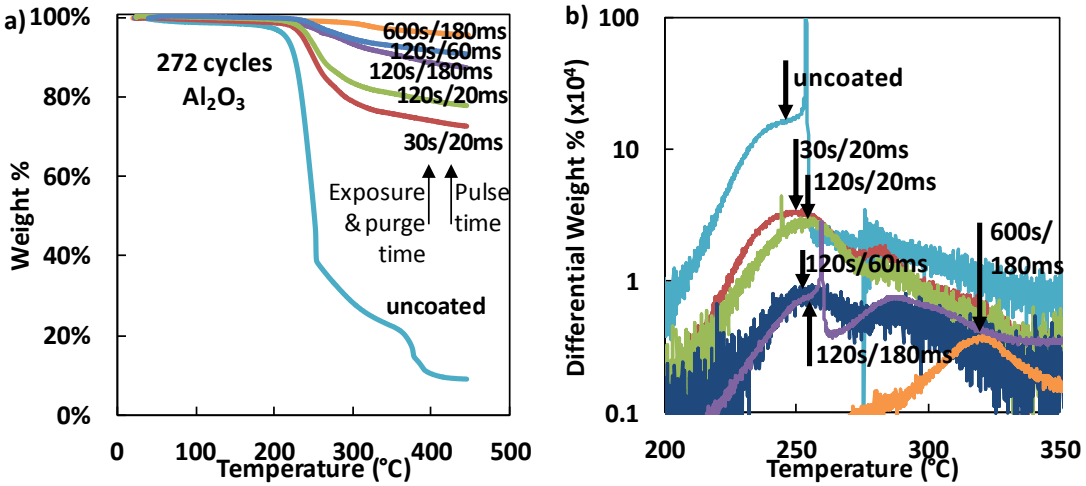

Figure 4: (a) TGA weight percent curves for CNC aerogels coated with 272 ALD cycles of Al_2O_3 with various pulse and exposure & purge times. (b) Plot of differential weight % vs. temperature for same data.

CONCLUSIONS

In this work, we formed an organic/inorganic nanocomposite by conformally coating CNC aerogel scaffolds with a thin layer of oxide. EPMA results showed Al_2O_3 penetration of

approximately 60 µm. SEM images indicated that the coating is conformal throughout the penetration depth. TGA showed that Al_2O_3 coatings are able to delay the onset of oxidation of the aerogel to above 300°C and that coatings deposited with longer exposure / purge times and longer pulse times are able to coat more of the aerogel and provide better protection against oxidation. It is anticipated that the hard, wear-resistant Al_2O_3 coating should result in a nanocomposite with improved mechanical properties, increased allowable processing temperature, and improved barrier properties. These properties along with their renewable nature should make CNC aerogels an attractive choice as a reinforcing fiber in polymers.

ACKNOWLEDGEMENTS

EMPA was carried out at the Electron Microprobe Laboratory in the College of Oceanic and Atmospheric Sciences at OSU. The authors acknowledge Dr. Yi Liu and Teresa Sawyer of the OSU Electron Microscopy Facility for their help with sample preparation and SEM analysis as well as Dr. Skip Rochefort for use of TGA. JFC was supported by NSF DMR 0805372 and SWS was supported by NSF CHE 1102637.

REFERENCES

1. R. J. Moon, A. Martini, J. Nairn, J. Simonsen, and J. Youngblood, Chem. Soc. Rev. **40**, 3941 (2011).
2. P. F. Carcia, R. S. McLean, B. B. Sauer, and M. H. Reilly, J. Nanosci. Nanotech. **11**, 7994 (2011) .
3. R. L. Puurunen, J. Appl. Phys. **97**, 121301 (2005).
4. J. T. Korhonen, P. Hiekkataipale, J. Malm, M. Karppinen, O. Ikkala, and R. H. A. Ras, ACS Nano **5**, 1967 (2011).
5. M. Kettunen, R. J. Silnennoinen, N. Houbenov, A. Nykanen, J. Ruokolainen, J. Sainio, V. Pore, M. Kemell, M. Ankerfors, T. Lindstrom, M. Ritala, R. H. A. Ras, and O. Ikkala, Adv. Funct. Mater. **21**, 510 (2011).
6. J. Biener, T. F. Bauman, Y. Wang, E. J. Nelson, S. O. Kucheyev, W. V. Hamza, M. Kemell, M. Ritala, and M. Leskelä, Nanotechnology, **18**, 055303 (2007).
7. S. Ghosal, T.F. Baumann, J.S. King, S. O. Kucheyev, Y. Wang, M.A. Worsley, J. Biener, S. F. Bent, and A. V. Hamza, Chem. Mater. **21**, 1989 (2009).
8. J.W. Elam, J. A. Libera, M. J. Pellin, A. V. Zinovev, J. P. Greene, and J. A. Nolen, Appl. Phys. Lett. **89**, 053124 (2006).
9. S. O. Kucheyev, J. Biener, Y. M. Wang, T. F. Baumann, K. J. Wu, T. Buuren, A. V. Hamza, J. H. Satcher, Jr., J. W. Elam, and M. J. Pellin, App. Phys. Let. **86**, 083108 (2005).
10. S. Noorani, J. Simonsen, and S. Atre, *ACS Symposium Series No. 938* (Oksman, K. & Sain, M., eds.) Amer. Chem. Soc., Washington, D.C. (2006)
11. A. C. Besemer, A. E. J. de Nooy, and H. van Bekkum, in *Cellulose Derivatives* (ACS Publications, 1998) p. 73.
12. P. L. Bragd, A. C. Besemer, and H. van Bekkum, J. Mol. Cat. A: Chem. **170**, 35 (2001).
13. A. E. de Nooy, A. C. Besemer, and H. van Bekkum, Carb. Research **269**, 89 (1995).
14. A. E. de Nooy, A. C. Besemer, H. van Bekkum, and J. A. P. van Dijk, Macromolecules, **29**, 6541 (1996).